10

Thermal Imaging for Enhancing Inspection Reliability: Detection and Characterization

Soib Taib[1], Mohd Shawal Jadin[2] and Shahid Kabir[3]
[1]*School of Electrical and Electronic Engineering*
USM Engineering Campus, Nibong Tebal
[2]*Faculty of Electrical and Electronic Engineering*
Universiti Malaysia Pahang, Pekan, Pahang
[3]*Sustainable Materials and Infrastructure Cluster*
Collaborative μ-Electronic Design Excellence Centre
Universiti Sains Malaysia, Nibong Tebal, P. Pinang
Malaysia

1. Introduction

Reliable performance of an equipment or structure depends on pre-service quality and in-service degradation of the equipment or structure under operating conditions. The role of non-destructive testing (NDT) is to ensure integrity, and in turn, reliability of equipment or structure. Besides, NDT can also monitor in-service degradation and to avoid premature failure of the equipments/structures and prevent accidents as well as save human life. Up to now, NDT has been used in various fields of applications such as the inspection of electrical power plant, substation, storage tanks, bridges, aircraft, pressure vessel, rail, pipeline and so on. Efficient and reliable NDT evaluation techniques are necessary to ensure the safe operation of complex parts and construction in an industrial environment for assessing service life, acceptability, and risk, as well as for reducing or even eliminating human error. Hence, making the inspection process to be fully automated could produce a more reliable, reproducible, faster evaluation and also sustainability.

Previously, due to the lack of effective computational and analytical tools, the data interpretation depends strongly on the experienced and expert of NDT personnel. Nonetheless, since the advancements in computer engineering, modern electronic systems, material science and other related fields made a major impact on all or many of the NDT methods. Data acquisition, analysis and interpretation were automated to increase the reliability and thus reduce the effect of human errors and wrong diagnosis. As NDT is not a direct measurement method, the nature and size of defects must be obtained through analysis of the signals obtained from inspection. Signal and image processing have provided powerful techniques to extract information on material characterization, size, defect detection, and so on. For instance, in the case of images, the major processing and analysis methods include image restoration and enhancement, morphological operators, wavelet transforms, image segmentation, as well as object and pattern recognition, facilitating extraction of special information from the original images, which would not, otherwise, be available. Therefore,

this chapter will emphasize the application of thermal image processing in assessing the reliability of concrete structure and diagnosing the condition of electrical equipments.

2. Infrared thermography

Infrared radiation was discovered in 1800 by William Hershel, who used a prism to refract sunlight onto thermometers placed just beyond the red end of the visible spectrum generated by the prism. He found that this area had the highest temperature of all, contained the most heat, and therefore contained a form of light beyond red light. Herschel's experiment was important, not only because it led to the discovery of infrared light, but because it was the first experiment that showed there were forms of light not visible to the human eye (Hellier, 2001).

2.1 IRT principles

Human eyes can only see light in the visible spectrum, ranging from about 400 nm to a little over 700 nm. The electromagnetic spectrum is a band of all electromagnetic waves arranged according to frequency and wavelength. As shown in Fig. 1, the wavelength spectrum of infrared light ranges from about 1 mm down to 750 nm. All objects emit energy proportional to its surface temperature. However, the energy radiated can only be detected by an infrared detector that depends on the emissivity coefficient of the surface under measurement.

The core of the camera is the infrared detector, which absorbs the IR energy emitted by the object (whose surface temperature is to be measured) and converts it into electrical voltage or current. Any object emits energy proportional to its surface temperature. However, the energy really detected (by the infrared detector) depends on the emissivity coefficient of the surface under measurement. The emissivity tells us how much of the thermal radiation from an object that is emitted due to the temperature of the object. All objects above absolute zero (0 Kelvin) emit infrared radiation. The Stefan-Boltzmann law describes the total maximum radiation that can be released from a surface. Since thermal imaging systems only respond to a small portion of the spectrum, it is necessary to introduce Planck's blackbody law.

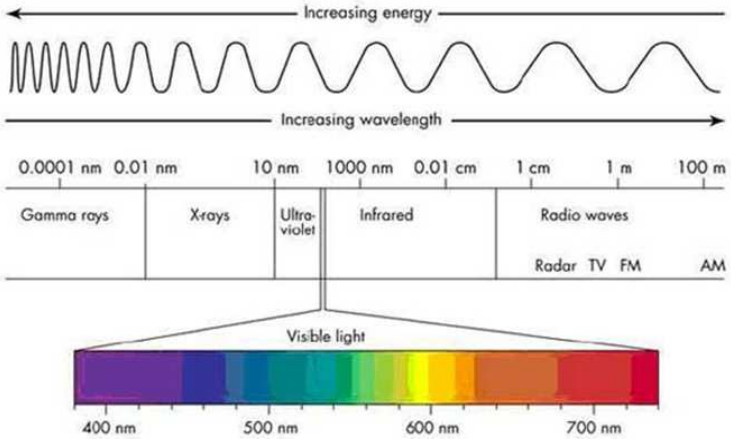

Fig. 1. Electromagnetic wavelength

Planck derived the law as in equation (1), which describes the spectral distribution of the radiation intensity from a black body where the emissivity of the surface, ε is equal to 1 (Holst, 2000).

$$\varepsilon_{\lambda b} = \frac{C_1}{\lambda^5 \left(e^{C_2/\lambda T} - 1 \right)} \quad \frac{W}{m^2 - \mu m} \tag{1}$$

where $\varepsilon_{\lambda b}$ is the black body monochromatic radiation intensity, C_1 (3.7411 x10^8 W-μm^4/m^2) and C_2 (1.4388 x10^4 μm-K) are the first and second radiation constants respectively; λ is the wavelength of the radiation being considered and T is the absolute temperature of the blackbody. By integrating Planck's law over the entire spectrum (λ = 0 to ∞), the total hemispherical radiation intensity is obtained.

$$\varepsilon_b = \sigma T^4 \tag{2}$$

where σ is the Stefan–Boltzmann constant (5.67051 x 10-8 W/m2K). It has to be pointed out that equation (2) describes the radiation emitted from a black body which is the maximum value radiated by a body at a given temperature. Real objects almost never comply with this law although they may approach the behaviour of a black body in certain spectral intervals. A real object generally emits only a part ε_λ of the radiation emitted by a black body at the same temperature and at the same wavelength. By introducing the quantity,

$$\varepsilon = \frac{\varepsilon_\lambda}{\varepsilon_{\lambda b}} \tag{3}$$

which is called the spectral emissivity coefficient, equation (2) can be rewritten for real bodies by simply multiplying its second term by ε_λ. When averaged over all wavelengths, the total power density for a non-black body object is

$$emissivity = \varepsilon \sigma T^4 \tag{4}$$

As infrared energy functions outside the dynamic range of the human eye, special equipment is needed to transform the infrared energy to another signal, which can be seen. For this purpose, infrared imagers were developed to see and measure this heat. There are two general types of infrared instruments that can be used for condition monitoring: infrared thermometers and infrared focal plane area (FPA) cameras (Braunovic, 2007). Infrared thermometers only provide a temperature reading at a single and relatively small point on a surface area. Another type of instrument that can provide a one-dimensional scan, or line of comparative radiation, is the line scanner. This type of instrument provides a somewhat larger field of view in predictive maintenance applications compared to the infrared thermometer (Mobley, 2002). Further advancements in infrared thermographic technology started with the development of the FPA. Based on FPA technology, nowadays various types of IR imagers with more advanced and sophisticated features have been developed (Epperly et al 1997). Although FPA technology is more expensive than infrared thermometers and line scanners, it provides more flexible and accurate measurements.

The basic concepts of the IR imager, commonly known as the thermographic camera, is that it can capture an image of the thermal pattern and measure the emissive power of a surface in an area at various temperature ranges. The digital output image of IRT is called a thermogram. Each pixel of a thermogram has the specific temperature value, and the image's contrast is derived from the differences in surface temperature. An infrared imaging system detects radiation in the infrared part of the electromagnetic spectrum and produces images from that radiation. All objects emit infrared radiation and the amount of emitted radiation increases with temperature. Therefore, infrared imaging allows us to see variations in temperature. In an infrared imaging system, there are two types of IR detectors i.e. mid wave (MW) and long wave (LW) which are operated in the range of 2–5 μm and 8–14 μm of the electromagnetic spectrum band, respectively (Minkina & Dudzik, 2009). These bands do not cover the full infrared spectrum because not all parts of the spectrum are suitable for infrared imaging. The reason for this is that the atmospheric transmission of infrared radiation is low in some ranges of the spectrum. This means that the atmosphere will block infrared radiation in these ranges, thus making these wavelengths unsuitable for infrared imaging. Most infrared cameras today work in the MW or LW ranges (Wretman, 2006). The energy detected depends not only on the emissivity coefficient of the surface under measurement but also on the environment. In fact, a fraction may be either absorbed by the atmosphere between the object and the camera, or added as reflected by the surface from the surroundings. This part will be discussed further in the following parts of this chapter.

2.2 Type of IRT

Infrared thermography is generally classified in two types, passive and active thermography (Kumar et al, 2009). In passive thermography, the temperature gradients are present in the materials and structures under tests naturally. In active thermography, the relevant thermal contrasts are induced by an external stimulus (Santos, 2008). The passive method has been widely applied in diverse areas such as production, predictive maintenance, medicine, detection of forest fire, thermal efficiency survey of buildings, road traffic monitoring, agriculture and biology, detection of gas and in NDT. In all these applications, abnormal temperature profiles indicate a potential problem to take care of.

In active infrared thermography, the sample is heated by an external controlled heat source and its surface temperature is monitored as a function of time through changes of emitted infrared radiation. The specific thermal properties of the material under test influence transport of heat thus causing surface temperature to change with respect to areas with different thermal properties. Active thermography is a very popular method in NDT applications such as for detecting crack in structure. There are many methods that have been used in active thermography. Table 1 shows the summary of active thermography methods and its characteristics (Maldague, 2000).

Contrary to active thermography, passive thermography approach does not require external heat source. This is because the heat flow necessary for the evaluation already exists naturally. Passive thermography only to pinpoints anomalies since the heating energy source is difficult to measure. Therefore the accuracy and reliability of passive thermography is not a major concern. In many applications, passive thermography applies relative temperature from the similar object or surrounding temperature. This is well known as qualitative measurement that will be discussed later. One of the applications of passive

Methods	Characteristic
Pulse Thermography (PT)	Fast inspection relying on a thermal stimulation pulse, with duration going from a few milliseconds for high thermal conductivity material inspection (such as metal parts) to a few seconds for low thermal conductivity specimens (such as plastics, graphite epoxy components).
Step Heating (SH)	Contrary to PT scheme for which the temperature decay is of interest (after the heat pulse), the increase of surface temperature is monitored during the application of a step heating pulse ('long pulse'). Variations of surface temperature with time are related to specimen features.
Lock-in thermography	Based on thermal waves generated inside the specimen under study in the permanent regime. Here, at a frequency, the specimen is submitted to a sine modulation heating, which introduces highly attenuated a dispersive thermal waves of frequency inside the material (in close to the surface region).
Vibrothermography	A mechanical vibration induced externally to the structure direct conversion from mechanical to thermal energy occurs and the heat is released by friction precisely at locations where defects such as cracks and desalinations are located.

Table 1. Method of active thermography

thermography is for preventive and predictive maintenance. In construction for example the passive thermography can be used in the search of hidden defects or damages in the road or bridge pavement structure, together with information on the degradation mechanism, serves as an early diagnostic tool, which completes the methodologies utilised for the survey of the state of the paving (Stimolo, 2003)

2.3 A Review of IRT applications

In electrical power systems, the developed IRT plays a vital role in inspecting and diagnosing the integrity of electrical power equipments. It has become one of the preferred methods for assessing equipment conditions online especially in electrical transmission and distribution systems (Lindquist & Bertling, 2008). IRT can be used to monitor the thermal behaviour of the power equipment, as well as the structure of a system. It senses the emission of infrared energy (i.e. temperature) to detect thermal anomalies, which are hotter or colder than they should be. Through this the inspector can then locate and identify the incipient problems within the system. While heat is not a perfect indicator of all problems in electrical systems, heat produced by abnormally high electrical resistance often precedes electrical failures (Hellier, 2001). Although the technique for inspecting electrical systems is quite straightforward, there are several things that need to be considered. Some of the factors, such as environmental effects and equipment conditions, will normally affect the analysis results, especially during an outdoor inspection of a power substation, for example. Direct inspection without considering these factors definitely will result in inaccurate measurements. A good electrical thermographer must contend with several problems related to the electrical equipments, the infrared instrument, and the interpretation of data.

2.3.1 Measurement and analysis methods

There are two ways for temperature measurement. The first is known as quantitative, which is to take the exact temperature values of the objects. The second type is qualitative, which takes the relative temperature values of a hotspot with respect to other parts of the equipment with similar conditions. Infrared thermography can be used as both a qualitative and a quantitative tool. Some applications do not require obtaining exact surface temperatures. In such cases, it is sufficient to acquire thermal signatures, which are characteristic patterns of relative temperatures of phenomena or objects. This method of qualitative visual inspection is expedient for collecting a large number of detailed data and conveying them in a fashion that can be easily interpreted. In contrast, accurate quantitative thermography demands a more rigorous procedure to extract valid temperature maps from raw thermal images (Griffit et al, 2001).

A widely used method of using thermography in electrical equipment inspection is by employing the ΔT criteria (Chou & Yao, 2009)(Lindquist et al., 2005). Qualitative measurements are sometimes called comparative thermography. When the comparative technique is used appropriately and correctly, the differences between the two (or more) samples will often be indicative of their condition (Hellier, 2001). The severity or the level of overheating of the electrical equipments will refer to the temperature-rating table. This table is usually divided into three or four different categories to indicate the maintenance priority based on the equipment's temperature rise with respect to other similar component (Lindquist et al., 2005). Table 2 shows the maintenance testing specifications for electrical equipment published by the InterNational Electrical Testing Association (NETA) ("Standard for Infrared Inspection of Electrical Systems & Rotating Equipment," 2008). NETA provides guidelines for thermal inspections of electrical equipment. These guidelines are based on differences in temperature from one phase conductor or component to another. Recommended action is dependent on the difference in the temperatures.

Priority	ΔT between similar components under similar load (°C)	ΔT over ambient temperature (°C)	Recommended Action
4	1 - 3	1 - 10	Possible deficiency, warrants investigation
3	4 – 15	11 - 20	Indicates probable deficiency; repair as time permits
2	---	21 – 40	Monitor until corrective measures can be accomplished
1	> 15	> 40	Major discrepancy; repair immediately

Table 2. Maintenance testing specifications for electrical equipment

Fig. 2 shows an example of a hotspot and its reference point. A hot area is the suspected component and the reference must be another similar component with the same condition. It could be similar components in other phases. In the ΔT method, the temperature differences between suspected and normal component is calculated as:

$$\Delta T = T_{hot} - T_{ref} \tag{5}$$

where T_{hot} is the warm or hot temperature value of the suspected components while T_{ref} is the reference temperature value from the normal operating component. The severity of the hot spot is then checked using Table 3 under the column 'ΔT between similar components under similar load (°C)'. Action should be taken according to the level of priority. The advantage of this practical method is to establish "failure" or "no failure" condition and the emissivity has only a minor impact on the result (Chou & Yao, 2009). A drawback is that the temperature tables are usually only found in handbooks and guidelines; which is not a standard benchmark. Moreover, the ΔT criterion does not say anything about whether the equipment temperature limits are actually exceeded and also will not expose systematic failures affecting all three phases' connection (Lindquist et al., 2005).

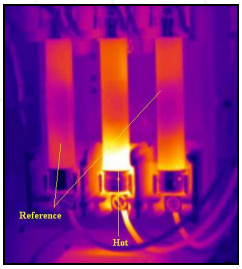

Fig. 2. Example of a hot fuse; the other fuses are used as the reference.

Environmental factor	Effect on IRT measurement
Ambient air temperature	An increase in air temperature will result in an increase in the measured temperature component. At a very high or very low-temperature, the IR system becomes less stable.
Precipitation/humidity (snow, rain, fog, etc.)	It can result in evaporative cooling. The temperature differences (either phase to phase or rise over ambient) can be dramatically reduced, leading to a misinterpretation of the data. Condition that is only slightly warm may be cooled below a point where they can be detected.
Wind or other convection	Wind speeds less than 5 mph can contribute to a significant cooling effect on a high resistance fitting. Wind speeds above 5 mph can reduce the temperature difference between the components and ambient to a few degrees above the ambient.
Sun or solar radiation	Solar heating of components, especially those with a high absorption of the sun's energy (such as aged conductors), will mask small thermal differences.

Table 3. Environmental factors effect on IRT inspection

In quantitative measurement, the reference is the ambient temperature. The observation is established by measuring the absolute temperature of electrical equipment under the same ambient conditions. As the reference temperature has to be measured, it requires an even greater understanding of the variables influencing radiometric measurement, as well as a grasp of its limitations. The temperature rise is calculated as:

$$\Delta T = T_{hot} - T_{amb} \tag{6}$$

where T_{hot} is the hot-spot temperature of the measured component and T_{amb} is the ambient temperature at the time of measuring. Again, the column 'ΔT over ambient temperature' in Table 3 is used for testing specifications.

2.3.2 Improving inspection techniques

Newer developments in modern IRT equipment have improved the quality of measurements. Most modern IR imagers can resolve surface temperature differences of 0.1°C or less (Hellier, 2001)(Griffith et al., 2001). An infrared thermographic system is essentially imaging IR radiometers that can provide IR images continuously and in real-time, just like the images provided by a normal video camera. Complete thermographic systems also integrate an advanced image processing and display system. Despite the advantage of modern designs of IRT cameras, there are still several factors that need to be considered when doing an inspection. Even if temperatures can be measured accurately, several other factors must be taken into account if the real influence of the abnormal temperature difference is to be accurately accounted for (Snell & Spring, 2003). This is a very critical aspect, especially for an outdoor inspection. The inspection of electrical power systems using IRT can be divided into three main areas; substation, underground distribution, and aerial distribution (Azmat & Turner, 2005). When accurate measurements are required, all the influence factors had to be identified during the IRT image is captured.

Generally, the factors that affect the accuracy of IRT measurements can be categorized as procedural, technical and environmental/ambient conditions (Santos et al., 2008)(Hellier, 2001). The procedural factor concerns the thermographer itself. This factor can be minimized if certified or qualified personnel are employed. For technical factors, the issue is normally relates to the emissivity of the equipment under inspection, load current variation, distance of the object being inspected, and the IRT camera specifications. For an outdoor or uncovered inspection, such as at a power substation, environmental effect is a critical issue. The data relates to the environmental factors are considered crucial and should be collected prior to inspection. Table 3 summarizes the environmental factors effects that need to be considered when doing an IRT inspection (Snell & Renowden, 2000).

A proper observation should be made before starting any IRT inspection. In most of the cases, essential information of the target location is provided. In this case, the history of the target location and electrical power equipments had to be considered. Among the important data needed for an inspection are the load variations, type of equipment and the materials used in building the. For an accurate measurement, the right and suitable tool should be selected. It is recommended that for an extensive outdoor inspection, especially during sunny periods, long-wave (generally 8 μm -14 μm) sensing of IRT systems should be used. It had been proven that within this wave band, the thermal detectors provide greater sensitivity to ambient temperature objects and insensitive to atmospheric attenuation (Balaras & Argiriou, 2002), (Epperly et al., 1997). Short-wave systems should be used only on a limited basis depend on the condition of loads and time (Hellier, 2001). In summary, Table 5 shows all the factors that can affect the IRT measurement related to the target equipment and the inspection tools.

3. Significance of imaging for inspection reliability

Digital signal and image processing is a widely used engineering term that, in a broad sense, can be described as a transformation converting signal data into useful information using digital computers. Although digital signal and image processing methods have been commonly employed in various scientific and engineering fields, their application in NDT is very recent. Back to the previous technique, NDT was implemented in a manual or semi-automatic method where the operator will accept or reject the decision. This approach is subject to error and wrong interpretation. Furthermore, most data recording and analysis methods are primitive. Therefore, utilizing the digital signal and image processing for the inspection can minimize the operator dependence because it uses automated data analysis, thus improving NDT inspection reliability. Both techniques can be employed to improve the signal-to-noise ratio (SNR) therefore increased the detection capabilities of the defect or fault. Detailed definitions of the detected problem such as type of defect, shape, size and severity of defects has acquired a great significance lately. This is because of the need for this information for implementation of such methodologies as retirement-for-cause and remaining-life analysis. In summary, applying automated imaging inspection can greatly improve the NDT inspection reliability including the use of non NDT technologies (Zu et all, 2011). Digital signal processing has played and will continue to play a very significant role in NDT. To provide a more complete understanding about this subject, the remainder of this chapter presents a deep review of how the IRT image processing technique can enhance and practically implemented for detecting and characterizing the inspection reliability of concrete structure and electrical equipment.

Since the early 1960s, infrared thermography (IRT) has been used in many fields of application, such as military, industrial, civil engineering and medical, as well as electrical engineering. IRT is a non-contact, non-destructive, visualizing technique, which is becoming an important means for quality control in production and in service inspection (Junyan et al., 2008). Due to its advantages in terms of being non-contact, free from electromagnetic interference, safe, reliable, providing large inspection coverage and fast data interpretation, IRT has taken a very important role in condition monitoring especially in predictive and preventive maintenance techniques (Azmat & Turner, 2005). Furthermore, inspections can be done without shutting down operation of the system.

4. Problem concerning faults and damage detection of power system equipment and concrete infrastructure

4.1 Fault diagnosis in power equipment

Electrical devices are usually rated in power, which indicates the maximum amount of energy the device can consume without being damaged. If the device operated above its specifications, the excess power causes the atoms present in the device's material to resonate and resist the flow of electricity. This resistance to the flow of electricity will generates heat, which in turn, overheats the device and reduces its life cycle and efficiency. Another major problem that usually created within the utility equipment is the change of resistance due to loose connections. The loose connection causes the electricity to occupy a smaller area of the defective connection that is required for proper flow. This phenomenon will and therefore increases the resistance and temperature of the connection. Any change in resistance will cause the equipment to consume more power than the intended load (Azmat & Turner, 2005). Fig. 3

shows an example of infrared image and the visual light image of a circuit breaker. The red colour region in the infrared image indicates the hot spot and possible anomaly.

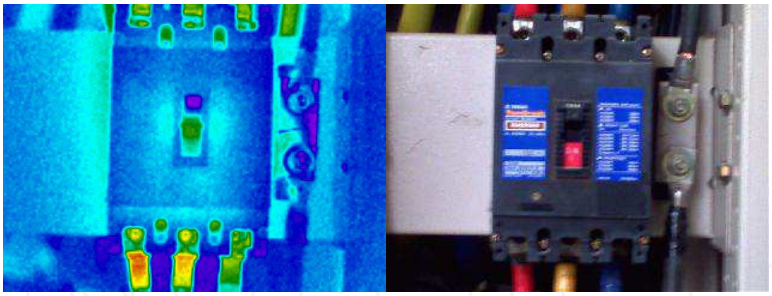

Fig. 3. Infrared image and visible light image

Faults in electrical power systems can be classified into a few categories, such as poor connection, short or open circuit, overload, load imbalance and improper component installation (Kregg, 2004),(Cao et al., 2008). In most cases, poor connections are among the more common problems in transmission and distribution lines of electrical power systems (Azmat & Turner, 2005). According to a thermographic survey conducted during the period of 1999-2005 (Martínez & Lagioia, 2007), it was found that 48% of the problems were found in conductor connection accessories and bolted connections. This is mainly due to loose connections, corrosion, rust, and non-adequate use of inhibitory grease. On the other hand, 45% of the thermal anomalies appear in disconnector contacts. Most of the anomalies are due to deformations, deficient pressure of contact, incorrect alignment of arms, and accumulation of dirt. Only 7% of the problems were found in electrical equipment. In diagnosing faults at power substation using IRT, it was found that transformers have taken priority over other equipment. This is due to the fact that transformers are the most costly equipment in a power substation. The common causes of failure in transformers are oil leakage and inferiority in internal insulation, which can lead to catastrophic destruction and power outage (Utami et al., 2009). For normal transformer installation, operating temperatures rise over ambient 65 ^{o}C for oil-filled and 150 ^{o}C air-cooled transformers respectively (Balaras & Argiriou, 2002). Temperatures above these operating points will cause breakdown in the insulation winding and therefore causing an electrical short-circuit.

By utilizing IRT, the thermal image will clearly indicate problem areas. The suspected areas then can be easily located and the problems indentified. Nevertheless, in some cases, the interpretation of thermographic images cannot be done directly except by an experienced and qualified thermographers because most of the thermographic characteristics had to be understood. According to (Hou, 1998), faults in electrical equipment can be divided into two kinds, external or internal, depend on location. However, internal faults are difficult to identify because they are much more complex. Table 4 summarizes the faults that commonly occur in electrical power equipments.

4.2 Automated diagnostic system

In industrial application, the sophisticated diagnosis system is the choice in order to get fast and accurate data with minimum maintenance cost. Most of the IRT cameras that are

Equipments	Common problem
Lightning arrestor, circuit breaker, disconnector, splices, transmission lines, compression clamps	Poor electrical connection: Loose, corroded or improper connection or splices. Poor breaker connection.
	Inoperative capacitor
	Fail lightning arrestor
	overloading
	Broken conductor strands
Bus duct	Unbalance load
	High resistance in joints
	Bus plug-ins
	Fuse connections
Switches, bus bars, capacitor bank, fuses, load centres, motor control centres	Poor electrical connection: Loose, corroded or improper connection and contacts.
	Unbalance load
	Harmonics, eddy currents and hysteresis
	Overloading
Transformer	Poor electrical connection: Loose, corroded or deteriorated connection.
	Unbalance load
	Overloading
	Low fluid level
	Overheated bushing
	Blocked cooling tubes
Motor and generators	Unbalance load
	Blocked cooling passage
	Shorted or open winding
	Overheating of brushed, slip rings and commutators.
	Overloading
Lighting	Poor electrical connection
	Overheating ballast

Table 4. Faults and their thermographic image characteristics

available today come with analysis software and have the capability to provide the inspection report. Furthermore, there is also stand-alone analysis software that can be used for any type of thermographic image. Digital images are uploaded into the computer directly from the IRT camera for further analysis. Most of the software may have various analysis functions, such as spot, area, isotherms, and line thermal measurements, as well as size measurements. Analysis can be extended beyond the image by displaying the numerical data in a spreadsheet or in various standard graphical forms, such as a histogram (Hellier, 2001). However, despite the power and ease of use of the software, the analysis process still needs qualified or experienced personnel. Also, most of the conventional analyses are time consuming in preparing the final report. Therefore, applying an intelligent system in thermographic image analysis can overcome this limitation. In recent years, rapid development in computer vision based on image processing techniques and the integration

of artificial intelligence has provided many advantages in monitoring and diagnosing problems. In electrical power systems, the application of IRT for automatic diagnosis using intelligent systems is still in the early stages.

This is due to the complex analysis and various factors that need to be considered in developing such system. Most of the research in automatic diagnosis of electrical power equipment and machine condition monitoring started in early 2000 and it become more complicated with the used of advanced materials. Table 5 shows the factors related to the target equipment and the inspection tool.

Equipments factor	Characteristic
Electrical loads	Temperature of the connection will increase as the load increases. For light load problems in the early stages of failure will be less thermally. It is recommended that during the inspection, the load on the line should be at least 40%.
Equipment emissivity	Most of the conductors have quite low emissivity, typically 0.1-0.3. While greasy, black, overheated and aged conductors can have emissivity values as high as 0.97, it is often difficult to assess this visually from a distance.
Thermal gradient	The heat of high resistance is usually being generated at some internal point to the surface. There exists a thermal gradient between the hottest spot inside the equipment and the surface being viewed.
IRT device (camera)	Factors that must be considered are resolution, both spatial and measurement, detected waveband, sensitivity as well as the signal processing speed.
Distance and angle	The resolution of the IRT image decreases with distance. Acute angles present less information than images taken at right angles.

Table 5. Factors related to the target equipment and the inspection tool

In order to automatically analyze the condition of electrical equipment, image processing techniques can be used to extract the thermal profiles within the electrical equipments. Image processing techniques generally consist of several steps: pre-processing, segmentation, feature extraction, classification and decision making. The straightforward approach is to follow these steps one by one in bottom-up order. There are three techniques that can be used to determine the thermal severity of electrical equipments through thermal image analysis. The first one is a direct interpretation by identifying the real maximum temperature for each of electrical equipment and evaluating their condition based on the ΔT criteria. The maximum temperature is determined by finding the highest pixel value within the selected region. Calculating the histogram or histogram distance is another method that can be used for finding the similarity between two objects. In this case, the histogram for each region is computed and compared with other regions in order to get the ΔT. Another approach is to analyze the gradient of the segmented region. One of the advantages of utilizing the gradient analysis technique is that the source of the hotspot in electrical equipment can be identified.

Based on previous research, the simplest method of identifying hotspot regions within a thermal image of electrical equipment is to use thresholding techniques (Chou & Yao,

2009),(de Oliveira & Lages, 2010). The hot spot area is detected by filtering the image using a certain threshold value. Then, the hotspot region is extracted using morphological segmentation where the maximum gray pixel value determines the maximum temperature of the hotspot region. The reference temperature is derived from the average gray values of the equipment outside of the hotspot region. The level of severity of the electrical equipment is calculated by comparing the hotspot temperature and the reference temperature (Chou & Yao, 2009)(de Oliveira & Lages, 2010) (Baoshu et al., 2006). In another approach, the watershed transformation algorithm is used for segmenting the hotspot regions in the thermal image of electrical equipment (Almeida et al., 2009).

For diagnosing the thermal fault within electrical equipment, certain feature descriptions are created for the regions of interest. For the classification process, various intelligent techniques, such as neuro-fuzzy (Almeida et al., 2009), artificial neural network (Shafi'i & Hamzah, 2010) and support vector machine (SVM) algorithm (Li et al., 2006)(Rahmani et al., 2010) are used to determine the condition of the electrical equipment. The thermal profiles of electrical equipment can also be extracted by analyzing their real temperature values. The real temperature values for each pixel in the image can be extracted directly from its RGB data. This method is quite straightforward but has a problem with high processing time due to the large feature vectors to be computed by an artificial neural network (ANN) algorithm (Shafi'i & Hamzah, 2010). The previous research with various hotspot detection techniques and fault classification method is summarized in Table 6.

Reference	Automatic hotspot detection technique	Fault classification method
(Ying-Chieh Chou & Yao, 2009), (de Oliveira & Lages, 2010)	Thresholding	Calculating and comparing the real temperature values
(Laurentys Almeida et al., 2009)	Watershed segmentation	Neuro-fuzzy
(Shafi'i & Hamzah, 2010)	RGB image data	ANN
(Baoshu Li et al., 2006), (Rahmani et al., 2010)	Thresholding	SVM
(Wretman, 2006),(Smedberg, 2006)	Finding repeated pattern and smooth but steep image gradient	ANN
(Korendo & Florkowski, 2001)	Manually find region	Invariant coefficient method
(Younus & Bo-Suk Yang, 2010)	discrete wavelet decomposition	Bio-orthogonal wavelet algorithm
(Wong, Tan, Loo, & Lim, 2009)	RGB	RGB value comparison

Table 6. Automatic Diagnosing System of Electrical Equipment

Based on previous research except (Almeida et al., 2009), most of the diagnoses systems are only analyze the captured thermal image without considering other important variables. In this research, the only thing that distinguishes this research from others is the input variables. Besides considering environmental factors, this study also includes the

identification variables of the electrical equipment, such as pollution index, rated voltage, material and manufacturer of the equipment. The whole system diagram and the input variables are depicted in Fig. 4(a) and Fig. 4 (b) respectively.

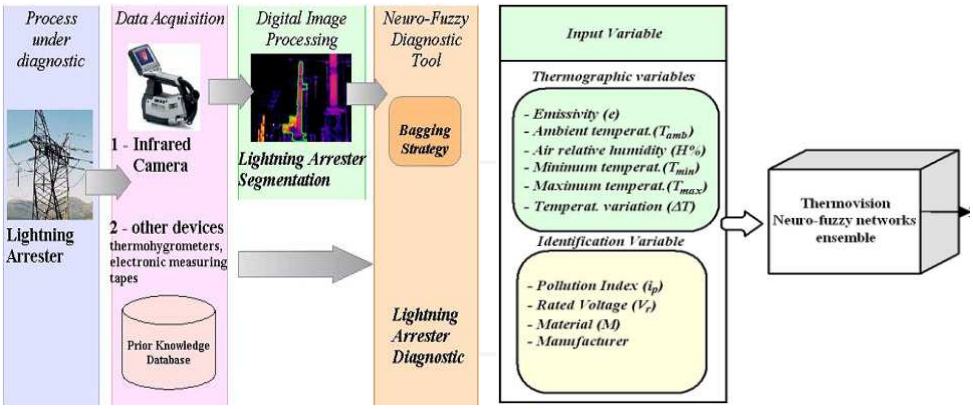

(a) (b)

Fig. 4. Intelligent surge arrester diagnosis system (a) system block diagram (b) input variables for neuro-fuzzy classifier

Instead of using classical bottom-up approach, Wretman (Wretman, 2006) and Smedberg (Smedberg, 2006) have successfully segmented the IRT image of electrical installation by using the top-down approach of image processing method. In other words, identifying the interesting region will be done first by detecting and grouping a regular repetitive structure. The tasks for finding repeated objects in the image can be broken down into two separate steps: (i) finding interesting features in the image and describing these using pre-specified descriptors, and (ii) comparing all the features and look for matches. In this research, all the interesting features were detected by modifying the scale-invariant feature transform (SIFT) algorithm (Lowe, 2004).

4.3 Damage detection of concrete infrastructure

The deterioration of concrete infrastructure is a growing problem worldwide; many structures are approaching the end of their service lives and need maintenance or rehabilitation in order to remain functional. In spite of recent increases in public infrastructure investments, infrastructure is deteriorating faster than it is being renewed. Various factors can contribute to the deterioration of concrete infrastructure; mechanical stress and fatigue, and chemical and environmental conditions are among the major causes concrete distress (Scott et al., 2003). Damage such as cracks, may exist in concrete even before the structure is subjected to any external loading. An excessive water-cement ratio, improper curing, and creation of high temperatures during the hardening process may result in shrinkage, which is the direct cause of cracking. These cracks later expand and widen during service due to freeze and thaw cycles and the intrusion of moisture. This process is especially critical for large concrete structures, such as dams, due to placement of massive amounts of concrete during construction. Even an initially sound concrete dam can develop cracks during its service life. Since a concrete dam is always in contact with water,

relatively small size cracks will eventually become wider and develop into holes or delaminations, and decompression joints or bedding in the shallow bedrock. Assessing the safety of concrete gravity dams against sliding requires a detailed investigation of the cracks and other discontinuities in the concrete structure and the rock foundation underneath. This is achieved through characterization of the mechanical properties of the materials (concrete and rocks), and especially the shear strength of the different types of discontinuities found throughout the structure and the foundation. Traditionally, a log is kept of the discontinuities found in cores drilled from the investigated structure. This method has the advantage of providing specimens for petrographic examinations and allows the testing of specific properties, such as compressive strength, Young modulus or permeability. However, information on the condition of the discontinuities is sometimes altered or lost due to drilling operations, even if a triple-tube coring system is used.

For instance, cracks might be created during drilling or transportation of the samples. Also, planes of cohesive weakness can separate after drilling, which modify the evaluation of the shear properties of the structure. The orientation of the core is another parameter that can be lost during drilling, if the procedure is not properly done. Since drilled cores are usually collected from dams for testing concrete and rocks, the borehole itself can be used to perform a detailed investigation and collect additional information on the surrounding materials. Borehole geophysical logs have been used for more than 50 years, mainly for oil mining. These methods provide continuous quantitative and statistical measurement of the depth, thickness, and orientation of features such as fractures and joints. Borehole imaging can actually provide better data than core samples, since the equipment used (the televiewers) depict in-situ conditions, and are not subjected to incomplete core recovery. Furthermore, tools are magnetically referenced to true north, thus eliminating the need for oriented cores.

Map-like surface cracking may indicate an adverse reaction between cementitious alkalis and aggregates. This reaction, known as the alkali-aggregate reaction (AAR) is a potentially harmful process in concrete containing reactive aggregates, and can lead to varying degrees of cracking in structures, as well as differential movement and misalignment of concrete elements and mechanical installations (Bérubé et al., 2000). AAR has been recognized in more than 50 countries around the world; it is likely that the problems associated with AAR exist in a larger number of countries, but concrete distress in several instances may have been attributed to other causes.

4.4 Advances in thermography imaging for sub-surface damage detection

Visual colour and greyscale imagery of concrete greatly extend natural vision capabilities in terms of colour and greyscale perception. Human vision is relatively poor at differentiating the brightness and colour features in the scene being viewed, whereas greyscale digital imagery can provide hundreds of levels of grey and colour digital imaging allows the quantitative differentiation of millions of different colours. Such a range of image perception is unattainable by the human eye, but is extremely useful for quantitative image analysis. There is, however, a need for the development of effective image analysis techniques in order to derive the information needed from the concrete imagery. Surface damage, such as cracks, are usually treated as objects, and are thus quantified through techniques that first segment the objects from the background to extract shape or object features, and then classify the images based on those features.

Visual colour and greyscale imagery of concrete greatly extend natural vision capabilities in terms of colour and greyscale perception. Human vision is relatively poor at differentiating the brightness and colour features in the scene being viewed,whereas greyscale digital imagery can provide hundreds of levels of grey and colour digital imaging allows the quantitative differentiation of millions of different colours. Such a range of image perception is unattainable by the human eye, but is extremely useful for quantitative image analysis. There is, however, a need for the development of effective image analysis techniques in order to derive the information needed from the concrete imagery. Surface damage, such as cracks, are usually treated as objects, and are thus quantified through techniques that first segment the objects from the background to extract shape or object features, and then classify the images based on those features.

A variety of image processing techniques can be used to characterize the damage in concrete data; among these methods are edge-detection algorithms (Abdel-Qader et al., 2003). Edges are considered to be areas with strong intensity contrasts in an image, causing a jump in intensity from 1 pixel to the next. In image data of damaged concrete, these edges would characterize boundaries between areas of sound concrete and deterioration, such as cracks. However, in their study on the classification of pits and cracks in corrosion images, Livens et al. (Livens et al., 1996) found that segmentation approaches worked well on individual images, but proved unsatisfactory when applied to a large set of samples due to the variability in the background. So they adopted a method based on the analysis of the textured appearance of the pits and cracks in the images, which was successfully employed to discriminate between the two types of damage. Furthermore, according to He and Wang (He & Wang, 1991), a good understanding or a more satisfactory interpretation of an image should include the description of both spectral and textural aspects of the image.

Other approaches used for damage characterization include transform-based techniques. Wavelet transforms are powerful tools often employed in image processing applications. The main advantage of this transform remains in its ability to locally describe signal frequency content. Through the wavelet transform (Ksantini, 2003), an image is decomposed into several high-frequency images containing wavelet coefficients representing details with increasing scale and different orientations (Foucher et al., 2001). More specialized methods that may be used to detect deterioration in concrete images are statistical-based approaches. These techniques allow for the analysis of the textural content in an image. Statistical texture methods analyse the spatial distribution of grey values by computing local features at each point in the image, and deriving a set of statistics from the distributions of the local features (Haralick, 1979).

Different types of concrete damage each have a specific texture typical of the type of deterioration, which should permit their discrimination through texture analysis methods. There are very few studies that have applied image processing techniques, such as texture analysis, to extract textural features in order to obtain concrete deterioration information from optical imagery. The analysis of concrete structure can be done by extracting the texture information through the grey level co-occurrence matrix texture analysis approach and the deterioration features in the concrete imagery is detected through the artificial neural network classifier in order to obtain more accurate damage characterization and assessment. These methods are applied to three types of concrete imagery, thermographic,

colour and greyscale digital imagery as shown in Fig. 5, in order to evaluate their effectiveness in providing surface damage information.

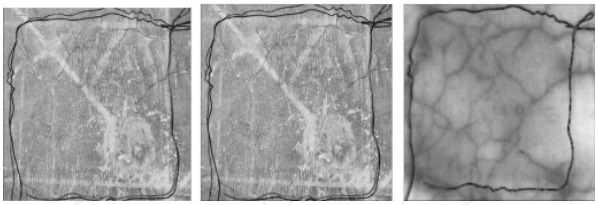

(a) (b) (c)

Fig. 5. Greyscale, thermographic, and colour images of GRAI-3 slab: (a) Greyscale, (b) Colour and (c) Thermographic.

Images were taken of concrete specimens exhibiting various levels of surface cracking associated with the alkali-aggregate reaction (AAR). This reaction occurs between some reactive aggregates and alkali hydroxides in the concrete pore solution. AAR leads to the swelling and cracking of concrete. The amount of cracking is closely related to the expansion level, and other indicators of concrete deterioration, such as loss of rigidity, decreasing mechanical properties, etc. (Rivard & Ballivy, 2005). Experiments were conducted on two sets of concrete specimens. The first set consists of three concrete blocks measuring 40×40×70 cm3 each, which were exposed outdoors to the elements for over ten years at the CANMET site in Ottawa (Canada); CAN-1, CAN-2, and CAN-3 present low, medium and high amounts of damage, respectively. The second set consists of three concrete slabs, 100×100×25 cm in size each, batched and kept at the GRAI laboratory (University of Sherbrooke). These slabs were wrapped with damp terry cloth and stored at ambient air (20±2 °C). As with the CANMET blocks, GRAI-1, GRAI-2, and GRAI-3 present low, medium and high amounts of damage, respectively. Table 7 and 8 provides more details on the concrete mixtures for the CANMET and GRAI specimens.

Concrete mixtures	**GRAI**			**CANMET**		
	GRAI-1	**GRAI-2**	**GRAI-3**	**CAN-1**	**CAN-2**	**CAN-3**
Cement content (kg/m³)	210	390	390	423	423	425
Density (kg/m³)	2223	2326	2340	2303	2303	2317
Total Na_2O_{eq} (kg/m³)	3.81	3.25	5.25	1.69	3.81	5.31
W/C	0.75	0.66	0.66	0.42	0.42	0.42

Table 7. Mixture proportions for CANMET and GRAI specimens.

Average measurement	GRAI			CANMET		
	GRAI-1	**GRAI-2**	**GRAI-3**	**CAN-1**	**CAN-2**	**CAN-3**
P-wave velocities (m s^{-1})[a]	3810	3590	3440	4909	4513	4402
Expansion (%)[b]	0.000	0.060	0.100	0.025	0.283	0.340

[a] Based on 11 measurements.
[b] Based on side and surface measurements.

Table 8. Average measurements of P-wave velocities and expansion levels

4.5 Statistical texture analysis using GLCM

Statistical texture methods analyze the spatial distribution of grey values in an image by computing local features at each point in the image, and deriving a set of statistics from the distributions of the local features. Depending on the number of pixels defining the local feature, statistical methods can be classified into first-order (one pixel), second-order (two pixels) and higher-order (three or more pixels) statistics. The outputs of the derived features are images in which the pixel values have been changed to reflect a particular feature, or texture; therefore, the resulting feature images are also known as texture features (Schowengerdt, 1997). A second-order histogram is an array that is formed based on the probabilities that pairs of pixels, separated by a certain distance and a specific direction, will have co-occurring grey levels. This array, or second-order histogram, is also known as the grey level co-occurrence matrix (GLCM). Since the co-occurrence matrix expresses the two-dimensional distribution of pairs of grey level occurrences, it can be considered a summary of the spatial and spectral frequencies of the image. A large number of texture features have been proposed; as many as fourteen different features that can be derived from these matrices are described by Haralick et al. (Haralick et all, 1973). However, only some of these are widely used. This is because many of the features are redundant, due to their high correlation. Thus they are not all useful for describing a particular texture. Some of the texture features that can be extracted from the GLCM are image contrast, correlation, dissimilarity, mean, variance, standard deviation, second moment, energy and entropy.

The most effective features are selected through a process consisting of visual analysis, histogram analysis, and analysis of correlation matrices. In this study, the thermographic image of the GRAI-3 slab, which exhibits a fair amount of deterioration associated with AAR and presents quite a bit of textural variation, was used in the feature selection process, since features found appropriate for this image will be suitable for the other images as well. For the first step in the feature selection process of the second-order statistics, visual analysis of the feature images revealed that the visual quality of the contrast and correlation features was not adequate; the contrast and correlation features were thus initially considered for discarding due to their poor quality in terms of visual information. This is shown in Fig 6.

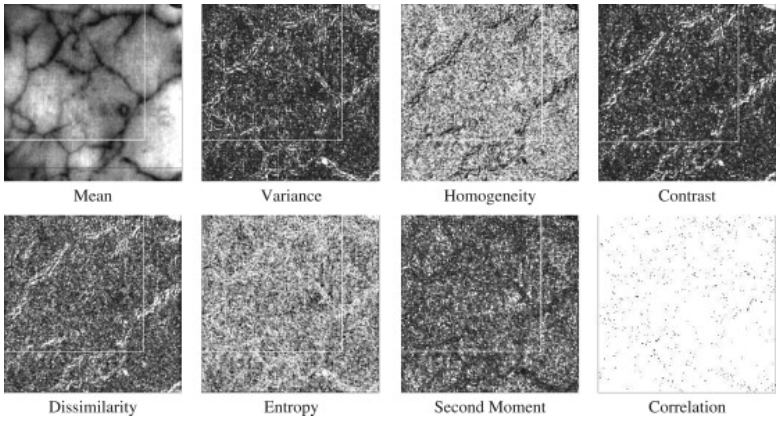

Fig. 6. Second-order texture features from green band of TIR G3 image.

Analysis of the histograms of the feature images confirmed that the two features, contrast and correlation, should be eliminated because of the narrow peaks they presented in their respective histograms, which signify a lack of textural information. The histogram of the variance feature also demonstrated a lack of texture information, so this feature was also considered for elimination (see Fig. 7).

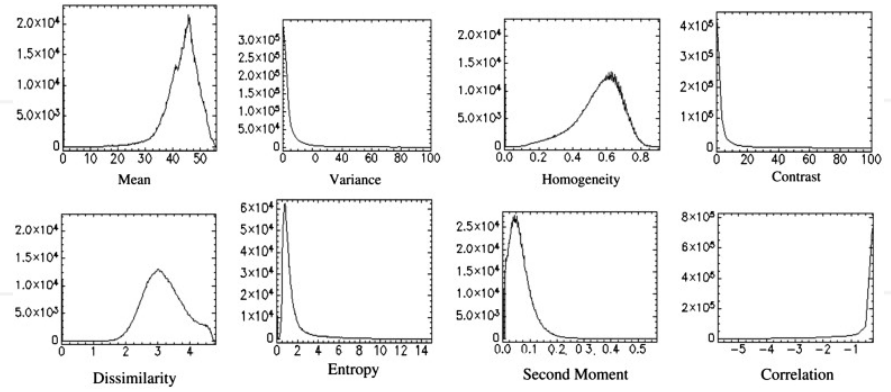

Fig. 7. Histograms of second-order features for greyscale map-crack image

Finally, the correlation matrix of the feature images was calculated; analysis of the correlation matrix further confirmed the removal of the contrast, correlation and variance features, due to their relatively high correlation with the other features. This analysis also indicated the need to discard the entropy and second moment features as well, due to the same reason (see Table 9). As a result, the mean, homogeneity and dissimilarity second-order features were selected for use in this study.

Features	Mean	Var	Homo	Cont	Diss	Ent	SM	Corr
Mean	1	−0.312	0.684	−0.240	−0.229	0.174	0.425	0.228
Var	−0.312	1	−0.515	0.833	0.857	0.500	−0.360	−0.376
Homo	0.684	−0.515	1	−0.512	−0.617	−0.324	0.797	0.450
Con	−0.240	0.833	−0.512	1	0.942	0.470	−0.338	−0.391
Diss	−0.229	0.857	−0.617	0.942	1	0.679	−0.486	−0.525
Ent	0.174	0.500	−0.324	0.470	0.679	1	−0.571	−0.454
SM	0.425	−0.360	0.797	−0.338	−0.486	−0.571	1	0.335
Corr	0.228	−0.376	0.450	−0.391	−0.525	−0.454	0.335	1

Table 9. Correlation matrix of second-order texture features for GRAI-3 thermographic image

The success of the GLCM method depends on the choice of the distance and the direction between the pixels, and the window size. The appropriate distance between pixels depends on how fine or coarse the texture of interest is. Small distances are usually used for fine textures since pixels close to each other will present enough variation in their grey values to characterize these textures, whereas greater pixel distances are generally used for more coarse textures because variations in the grey values occur in pixels farther away from each

other. It has been found that small distances produce the best results (Karathanassi, Iossifidis, & Rokos, 2000), since they are appropriate for textures that are fine, as well as for those that are coarse. A distance of 1 pixel means that the pixels in the pair are located right next to each other. Concerning the direction between pixels, four directions can be used: 0° (horizontal), 45° (diagonal), 90° (vertical) and 135° (diagonal); however, selecting which direction to use can be difficult. One method consists of calculating the GLCM features for all four directions and then taking their averages. The most common choice for the direction between pixels found in the literature, however, is 0°; this means that the pixels in the pair are located horizontally with respect to each other.

After extraction of the textural information from the images, the next step consists of classifying and quantifying the different classes of texture. Artificial neural networks (ANNs) classification approach based on MLP architecture was used to extract the crack patterns from the concrete imagery. Four input nodes were used to represent the following four input features: the original input image and the three selected second-order features. Three output nodes were used to correspond to the following three target classes: wide crack, narrow crack and no crack. For the training algorithm, the popular error back-propagation method was employed. In order to avoid poor classifications or inaccurate estimates of the elements, efforts were made to choose a sufficient number of training pixels for each class, in order to ensure adequate representation. After regions of the image were selected as training data and separate areas were selected as testing data, the software implemented the MLP, which then performed a classification using the four input features. This was done for each of the three image types, thermographic, colour and greyscale, of the CANMET and GRAI specimens. The results of the classification can be presented in two forms: a classified image (also known as a thematic map) which shows the spatial distribution of the various classes in which each pixel is assigned a symbol or colour that relates it to a specific class, and a table that summarizes the number of pixels in the whole image that belongs to each class. The Kappa coefficient was adopted to assess the accuracy of the results obtained.

Results of the classifications show that the greyscale imagery performed fairly well, with an overall classification accuracy range of 72.3–76.5% for the CANMET blocks, and 68.7–75.3% for the GRAI slabs. Classifications using the colour imagery were slightly better than the greyscale imagery, with accuracies ranging from 71.4% to 75.2% for CANMET blocks and 70.9–72.0% for the GRAI slabs. The thermographic imagery, however, produced the highest overall classification accuracies, which range from 73.1% to 76.3% for the CANMET blocks and 74.2–76.9% for the GRAI slabs. [Table 10] and [Table 11] show the classification accuracies obtained for each class, as well as the Kappa coefficients and overall accuracies for each specimen of the CANMET blocks and GRAI slabs, respectively. Fig. 8 presents the classified images for the greyscale, colour and thermographic imagery of the GRAI-3 slab.

Since the infrared thermography performed better than the other two types of imagery, only the results obtained from the thermographic image classifications were used to determine the various levels of AAR damage. The tabular results of the classifications performed on the thermographic imagery of the specimens are presented in Table 12. Among the CANMET blocks, specimen 1 presented the least amount of surface deterioration at 3.9% in the form of narrow cracks, specimen 2 had a moderate amount of narrow cracks (8.2%) and wide cracks (3.6%) for a total of 11.8% surface deterioration, and specimen 3 revealed the

	Thermographic			Colour			Greyscale		
	1	**2**	**3**	**1**	**2**	**3**	**1**	**2**	**3**
Kappa coefficient	0.73	0.73	0.74	0.69	0.71	0.74	0.74	0.73	0.76
Overall accuracy (%)	74.5	73.1	76.3	71.4	75.2	74.1	72.3	76.5	75.4
Classes	Accuracy (%)								
Wide crack	81.3	79.9	83.5	78.6	78.1	78.4	76.8	78.1	78.4
Narrow crack	79.7	78.6	81.5	77.7	70.9	77.5	76.3	70.9	77.5
No crack	82.4	76.7	80.6	75.3	74.5	74.2	73.6	71.4	74.2

Table 10. Classification accuracies for CANMET blocks

	Thermographic			Colour			Greyscale		
	1	**2**	**3**	**1**	**2**	**3**	**1**	**2**	**3**
Kappa coefficient	0.75	0.74	0.76	0.72	0.74	0.74	0.69	0.72	0.74
Overall accuracy (%)	75.6	76.9	74.2	70.9	71.6	72.0	68.7	74.1	75.3
Classes	Accuracy (%)								
Wide crack	76.7	78.1	80.0	73.4	76.1	79.9	70.4	77.1	79.7
Narrow crack	74.7	75.2	73.4	70.1	72.9	73.4	73.7	72.9	73.4
No crack	76.6	74.9	79.1	72.6	76.4	78.2	73.9	71.4	77.0

Table 11. Classification accuracies for GRAI slabs

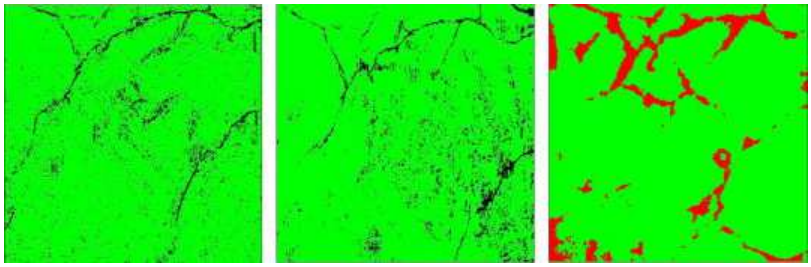

(a) (b) (c)

Fig. 8. Classified images of greyscale, colour and TIR images of GRAI-3 specimen: (a) Greyscale classified, (b) Colour classified and (c) TIR classified.

greatest amount of narrow cracks at 19.7%, as well as a number of wide cracks at 14.3%, for a total surface deterioration of 34.0%. For the GRAI slabs, specimen 1 had a total surface damage of 1.14% comprised of narrow cracks, specimen 2 presented 14.1% total damage made up of 8.8% narrow cracks and 5.4% wide cracks, and specimen 3 showed 14.0% narrow cracks and 9.1% wide cracks for a total surface deterioration of 23.1%.

Further analysis of the surface damage was performed after converting the classified images into binary images. This process simplifies the image by assigning the pixels that represent a damage value of 1 (black) and the background pixels a value of 0 (white). Manual or automated methods are then used to count or sum the pixels to calculate total crack length, as well as average crack width. In order to quantify the total length of wide cracks, pixels

Specimens	Classes	CANMET		GRAI	
		Image pixels	Image (%)	Image pixels	Image (%)
3	Wide crack	37 356	14.3	23 907	9.1
	Narrow crack	51 852	19.7	36 674	14.0
	No crack	172 936	66.00	201 563	90.3
	Total pixels	262 144	100.00	262 144	100.00
2	Wide crack	9 489	3.6	14 078	5.4
	Narrow crack	21 365	8.2	22 937	8.8
	No crack	231 290	88.2	225 129	85.8
	Total pixels	262 144	100.00	262 144	100.00
1	Wide crack	0	0.00	0	0.00
	Narrow crack	10 119	3.9	5 943	1.1
	No crack	252 025	96.1	256 201	98.9
	Total pixels	262 144	100.00	262 144	100.00

Table 12. Tabular representation of thermographic classifications

along the length of each branch of the cracks were summed and the total multiplied by the pixel resolution of 0.26 mm. For the CANMET blocks, a total length of 237.4 mm of wide cracks was calculated for specimen 3. For specimen 2, the total length was found to be 97.6 mm, and for specimen 1, the total length was 0 mm. Determination of average crack width was done by measuring the width of the wide cracks at several points. Each square represents one pixel at a resolution of 0.26 mm. As a result, the average width of cracks in the CANMET blocks was found to be 1.6 mm for specimen 3, 0.8 mm for specimen 2, and 0 mm for specimen 1.

These findings are supported by in-situ data recorded for the CANMET blocks and the GRAI slabs. CAN-3 was prepared with the highest alkali content, and showed the highest expansion level. On the other hand, CAN-1 showed the lowest expansion level as the concrete was mixed with a low level of alkali content. The highest values for the total length of wide cracks as well as for the average width of cracks found for the CAN-3 specimen also relate well to its having the lowest P-wave velocities (Table 8), indicating the highest deterioration level. The absence of wide cracks in the CAN-1 sample, which had a value of 0 mm for the average width of cracks, as well as for the total length of cracks, corresponds well to the lower percentage for average expansion levels measured on the blocks, where the CAN-2 sample showed a higher percentage, and with the CAN-3 sample having the highest percentage of expansion.

As for the GRAI slabs, the absence of wide cracks in the GRAI-1 specimen, which had a value of 0 mm for the average width of cracks, as well as for the total length of cracks, is corroborated by its having the lowest expansion level, indicating very little damage. A higher level of expansion was measured on the GRAI-2 specimen, with the GRAI-3 specimen having the highest measurement for expansion level among the slabs. Fig. 9 demonstrates the relationship between the test measurements and the damage quantities obtained for the three CANMET blocks and the three GRAI slabs. Fig. 9(a) presents a comparison of the total amount of crack damage and expansion levels, Fig. 9(b) is a comparison of the total crack length and expansion levels, and Fig. 9(c) is a comparison of total crack damage and P-wave velocities.

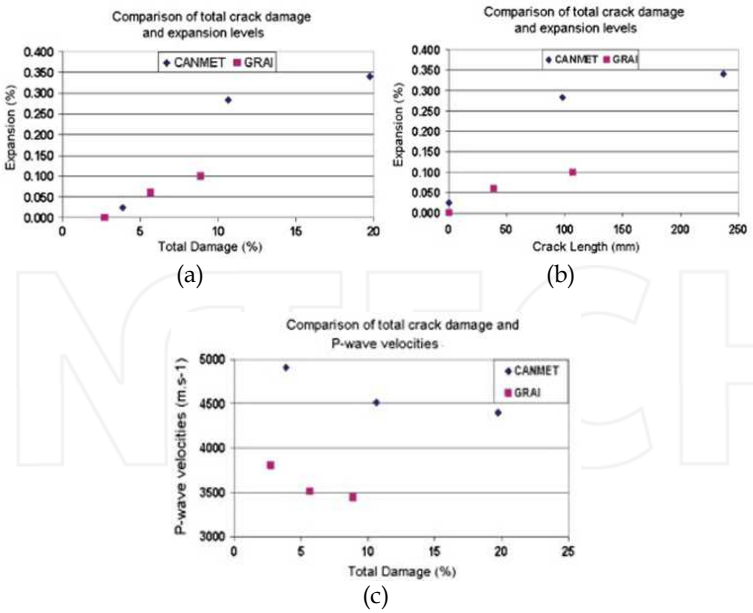

Fig. 9. Comparison of test measurements and damage information: (a) Crack damage vs expansion levels, (b) Crack length vs expansion levels and (c) Crack damage vs P-wave velocities

5. Recommendations for future research and development

There are many things that need to be done in improving the quality of NDT inspections using IRT. This includes the technology of IRT equipment, method of inspection, advanced methods of fault diagnosis and so on. Of course, this will involve various fields of study. Since the demand for NDT inspection reliability and condition monitoring is increasing, a robust and rapid analytical tool is required to do inspections. This part will highlight some recommendations for future research in order to improve the reliability inspection. The main factor that mostly affects the quality of inspection is the IRT equipment itself. Advances in manufacturing processes of thermographic detectors have dramatically increased both yield and quality while reducing production costs. However, the quality of inspection is related to the image resolution. Poor resolution will produce bad interpretation of inspection images. Therefore, for more accurate and correct data interpretation, it is recommended to use the latest technology for IRT cameras. Besides the resolution, the modern IRT cameras have very high thermal sensitivity. Some cameras even have the capability to adjust data measurements on screen, like object emissivity, temperature, etc.

In monitoring the condition of electrical equipments, the adoption of continuous thermal imaging can deliver increased benefits over periodic thermal inspection, especially in respect of mission critical electrical equipment. There is a big advantage to continuous thermal monitoring, since faults can occur at any time. In addition, it is not operator dependent, nor is it dependent on the time of inspection, which is usually when the

equipment is running at load. Another benefit of real-time continuous monitoring is that the system can give warning signals or alarms if anomalies occur at any time. Therefore, action can be taken immediately. Perhaps one of the most important advantages of continuous monitoring is the ability to integrate continuous monitoring into existing Supervisory Control and Data Acquisition (SCADA) systems, enabling real-time remote monitoring without the need for separate systems or reports, which is something that cannot be achieved with periodic thermal inspections. Real-time imaging systems are not only rapid, compact and frequency agile, but they also have greater resolution, which improves imaging analysis and recording capabilities. Due to the high demand for preventive maintenance in electrical power systems, there is a need to have more reliable and robust intelligent systems. To date, most of the developed intelligent systems could not be used for all types of electrical equipments. This is due to the different features of the equipments. Therefore, a new intelligent system model has to be developed. Another issue in vision technology is the image quality. For inspections being done outdoors, the captured image will normally be affected by noise. Therefore, further study is needed on more advanced image processing techniques and developing new algorithms that could solve these problems.

Specifically in analyzing the civil concrete structure, studies can be conducted in order to determine which bands of RGB are more suitable for these two types of images in an effort to reduce the number of features that need to be computed, and results compared with those of greyscale imagery to see if there is any significant difference. Other topics for future studies can also be considered. One topic concerns the application of the statistical analysis. This research dealt with only first-order and second-order statistics; higher-order statistics were not commonly employed with remote-sensing imagery previously due to the computational costs involved when working with large image dimensions. Since concrete imagery has relatively much smaller image dimensions, and computer efficiency has steadily increased, the use of third-and higher-order statistics for the texture analysis of concrete imagery can also be further experimented.

Another subject is the development of a standard set-up for data acquisition, which would control the resolution and uniformity of large-scale data. Additional studies can comprise the development of a model for incorporating concrete image data from various NDT imaging techniques, such as optical images, which present image data of the surface, infrared thermography and acoustics, which are used for subsurface conditions, and ground penetrating radar, which is employed to obtain below-surface information of a structure. Furthermore, the image analysis model employed in this research has the potential to be developed as a component for automated damage assessment, which can be incorporated into a structural health monitoring system for concrete infrastructure. Automation of the system would allow for the assessment of a large volume of data, which could be used to establish a database of monitoring imagery, inspection results, etc. Since the imaging and inspection data can be stored in a digital format, image and data retrieval using metadata and content-based methods can be employed in order to compare the damage characteristics with previous inspection results and information. Data concerning a particular structure can be put together to form a three-dimensional representation of the condition using GIS techniques. This can aid in monitoring the condition of a structure; a history of inspection results can thus be examined and compared in order to quantitatively establish changes that occur with time.

6. Conclusion

In this chapter we covered briefly fundamentals of IRT imaging in NDT for enhancing the inspection reliability for both applications in monitoring the condition of electrical power equipment and damage detection in concrete structure. Inspection by utilizing thermal imaging especially for analyzing electrical installations and concrete structures presents many challenges due to the fact that these equipments and materials are non-homogeneous images. Some improvements in analysis methods need to be considered in order to avoid misinterpretation or inaccurate analysis of IRT data. Recent trends in IRT inspection showed that there is a need to apply an automatic intelligent system. A more advanced system could improve the quality of inspections. Therefore, some effort must be made to design a new approach of IRT inspection and to develop a better model for an intelligent system. For more complex image analysis, more robust and effective image processing techniques must be applied. Further development could enhance automatic processing capabilities in the form of automatic recognition of the measured objects and their critical parts.

7. Acknowledgment

This research was supported by Fundamental Research Grant Scheme (FRGS), Universiti Sains Malaysia (USM) and Universiti Malaysia Pahang (UMP).

8. References

Abdel-Qader, I., Abudayyeh, O., & Kelly, M. E. (2003). Analysis of Edge-Detection Techniques for Crack Identification in Bridges. *Journal of Computing in Civil Engineering*, Vol.17, No.4, pp.255.

Azmat, Z., & Turner, D. J. (2005). Infrared thermography and its role in rural utility environment. *Proceedings of Rural Electric Power Conference*, pp. B2/1-B2/4.

Balaras, C. A., & Argiriou, A. A. (2002). Infrared thermography for building diagnostics. *Energy and Buildings*, Vol.34, No.2, pp. 171-183.

Baoshu Li, Xiaohui Zhu, Shutao Zhao, & Wendong Niu. (2006). HV Power Equipment Diagnosis Based on Infrared Imaging Analyzing. *Proceedings of International Conference on Power System Technology*, pp. 1-4.

Bérubé, M.-A., Durand, B., Vézina, D., & Fournier, B. (2000). Alkali-aggregate reactivity in Québec (Canada). *Canadian Journal of Civil Engineering*, Vol.27, No.2, pp. 226-245.

Braunovic, M. (2007). *Electrical contacts fundamentals, applications and technology*. CRC Press, ISBN 9781574447279, Boca Raton.

Cao, Y., Gu, X.-ming, & Jin, Q. (2008). Infrared technology in the fault diagnosis of substation equipment. *Proceedings of 2008 China International Conference on Electricity Distribution,* pp. 1-6, Guangzhou, China.

Epperly, R. A., Heberlein, G. E., & Eads, L. G. (1997). A tool for reliability and safety: predict and prevent equipment failures with thermography. *Petroleum and Chemical Industry Conference, 1997. Record of Conference Papers. The Institute of Electrical and Electronics Engineers Incorporated Industry Applications Society 44th Annual*, pp. 59-68.

Foucher, S., Benie, G. B., & Boucher, J.-M. (2001). Multiscale MAP filtering of SAR images. *IEEE Transactions on Image Processing*, Vol.10, No.1, pp. 49-60.

Griffith, B., Türler, D., & Goudey, H. (2001). *Infrared thermographic systems: A review of IR imagers and their use*. Berkeley CA: John Wiley and Sons.

Haralick, R.M. (1979). Statistical and structural approaches to texture. *Proceedings of the IEEE*, Vol.67, No.5, pp. 786-804.

Haralick, Robert M., Shanmugam, K., & Dinstein, I. (1973). Textural Features for Image Classification. *IEEE Transactions on Systems, Man, and Cybernetics*, Vol.3, No.6, pp. 610-621.

He, D.-C., & Wang, L. (1991). Texture features based on texture spectrum. *Pattern Recognition*, Vol.24, No.5, pp. 391-399.

Hellier, C. (2001). *Handbook of Nondestructive Evaluation* (1st ed.). McGraw-Hill Professional. ISBN 0070281211

Holst, G. (2000). *Common sense approach to thermal imaging*. SPIE Optical Engineering Press. ISBN 9780819437228, Bellingham Wash.

Junyan, L., Jingmin, D., Yang, W., Hui, L., & Zijun, W. (2008). An IR lock-in thermography nondestructive test system Based on the image sequence processing. *Proceedings of 17th World Conference on Nondestructive Testing*. Shanghai, China.

Karathanassi, V., Iossifidis, C., & Rokos, D. (2000). A texture-based classification method for classifying built areas according to their density. *International Journal of Remote Sensing*, Vol.21, No.9, pp. 1807-1823.

Korendo, Z., & Florkowski, M. (2001). Thermography based diagnostics of power equipment. *Power Engineering Journal*, Vol.15, No.1, pp. 33-42.

Kregg, M. A. (2004). Benefits of using infrared thermography in utility substations. *Thermosense XXVI*, pp. 249-257,Orlando, FL, USA.

Ksantini, R. (2003). *Analyse multirésolution et recherche d'images.* M.Sc. Thesis, University of Sherbrooke, Sherbrooke, Québec, Canada.

Laurentys Almeida, C. A., Braga, A. P., Nascimento, S., Paiva, V., Martins, H. J. A., Torres, R., & Caminhas, W. M. (2009). Intelligent Thermographic Diagnostic Applied to Surge Arresters: A New Approach. *IEEE Transactions on Power Delivery*, Vol.24, No.2, pp. 751-757.

Lindquist, T. M., Bertling, L., & Eriksson, R. (2005). Estimation of disconnector contact condition for modelling the effect of maintenance and ageing. *in Power Tech, 2005 IEEE Russia*, pp. 1-7.

Lindquist, T. M., & Bertling, L. (2008). Hazard rate estimation for high-voltage contacts using infrared thermography. *Proceedings of Reliability and Maintainability Symposium*, pp. 231-237.

Livens, S., Scheunders, P., Van de Wouwer, G., Van Dyck, D., Smets, H., Winkelmans, J., & Bogaerts, W. (1996). A Texture Analysis Approach to Corrosion Image Classification. *Microscopy, microanalysis, microstructures*, Vol.7, pp. 143-152.

Lowe, D. G. (2004). Distinctive Image Features from Scale-Invariant Keypoints. *International Journal of Computer Vision*, Vol.60, No.2, pp. 91-110.

Maldague, X. (2000). Applications Of Infrared Thermography In Nondestructive Evaluation. *Trends in Optical Nondestructive Testing (invited chapter)*. Available from http://citeseerx.ist.psu.edu/viewdoc/summary?doi=10.1.1.33.2908

Martínez, J., & Lagioia, R. (2007). Experience performing infrared thermography in the maintenance of a distribution utility. *Proceedings of 19th International Conference on Electricity Distribution*, Vienna: CIRED.

Minkina, W., & Dudzik, S. (2009). *Infrared Thermography*. John Wiley & Sons, Ltd. ISBN 9780470682234, Chichester, UK

Mobley, R. (2002). *An introduction to predictive maintenance*. Butterworth-Heinemann, ISBN 9780750675314, Amsterdam;New York.

Niancang Hou. (1998). The infrared thermography diagnostic technique of high-voltage electrical equipments with internal faults. *Proceedings of 1998 International Conference on Power System Technology*, Vol.1, pp. 110-115.

de Oliveira, J. H. E., & Lages, W. F. (2010). Robotized inspection of power lines with infrared vision. *Proceedings of 2010 1st International Conference on Applied Robotics for the Power Industry (CARPI 2010)*, pp. 1-6, Montreal, QC, Canada.

Rahmani, A., Haddadnia, J., & Seryasat, O. (2010). Intelligent fault detection of electrical equipment in ground substations using thermo vision technique. *Proceedings of 2010 2nd International Conference on Mechanical and Electronics Engineering*, Vol. 2, pp. V2-150-V2-154.

Rivard, P., & Ballivy, G. (2005). Assessment of the expansion related to alkali-silica reaction by the Damage Rating Index method. *Construction and Building Materials*, Vol.19, No.2, pp. 83-90.

dos Santos, L., Bortoni, E. C., Souza, L. E., Bastos, G. S., & Craveiro, M. A. C. (2008). Infrared thermography applied for outdoor power substations. *Thermosense XXX,* Vol.6939, pp. 69390R-11). Orlando, FL, USA.

Schowengerdt, R. A. (1997). *Remote Sensing, Second Edition: Models and Methods for Image Processing*. Academic Press. ISBN 0126289816.

Scott, M., Rezaizadeh, A., Delahaza, A., Santos, C. G., Moore, M., Graybeal, B., & Washer, G. (2003). A comparison of nondestructive evaluation methods for bridge deck assessment. *NDT & E International*, Vol.36, No.4, pp. 245-255.

Shafi'i, M. A., & Hamzah, N. (2010). Internal fault classification using Artificial Neural Network. *Proceedings of 2010 4th International Power Engineering and Optimization Conference*, pp. 352-357.

Smedberg, M. (2006). *Thermographic Decision Support – Detecting and Classifying Faults in Infrared Images*. M.Sc Thesis. Royal Institute of Technology, Stockholm, Sweden.

Snell, J., & Renowden, J. (2000). Improving results of thermographic inspections of electrical transmission and distribution lines. *Proceedings of IEEE 9th International Conference on Transmission and Distribution Construction, Operation and Live-Line Maintenance Proceedings*. pp. 135-144.

Snell, Jr., & Spring, R. W. (2003). The new approach to prioritizing anomalies found during thermographic electrical inspections. *Thermosense XXV*, Vol.5073, pp. 222-230, Orlando, FL, USA.

Standard for Infrared Inspection of Electrical Systems & Rotating Equipment. (2008). Infraspection Institute. Available from http://www.armco-inspections.com/ files/ir/-Electrical%-20Rotating%-20Std.pdf

Stimolo M (2003), Passive infrared thermography as inspection and observation in bridge and road construction, International Symposium NDT-CE, Available from www.ndt/articleindice03/papers/v083.htm

Utami, N. Y., Tamsir, Y., Pharmatrisanti, A., Gumilang, H., Cahyono, B., & Siregar, R. (2009). Evaluation condition of transformer based on infrared thermography results.

Proceedings of 2009 IEEE 9th International Conference on the Properties and Applications of Dielectric Materials. pp. 1055-1058, Harbin, China.

Verma Anuj Kumar, Ray, A. K., Singh, S. P., Banerjee, D., & Schabel Samuel. (2009). A Review of Recent Advances in the Use of Thermography in Pulp and Paper Industry. *Indian Pulp and Paper Technical Association (IPPTA)*, Vol.21, No.2, pp. 55-58.

Wong, W. K., Tan, P. N., Loo, C. K., & Lim, W. S. (2009). An Effective Surveillance System Using Thermal Camera. *Proceedings of 2009 International Conference on Signal Acquisition and Processing*, pp. 13-17, Kuala Lumpur, Maylaysia.

Wretman, D. (2006). *Finding Regions of Interest in a Decision Support System for Analysis of Infrared Images*. M.Sc Thesis). Royal Institute of Technology, Stockholm, Sweden.

Ying-Chieh Chou, & Yao, L. (2009). Automatic Diagnostic System of Electrical Equipment Using Infrared Thermography. *Proceedings of International Conference of Soft Computing and Pattern Recognition*, pp. 155-160.

Younus, A. M., & Bo-Suk Yang. (2010). Wavelet co-efficient of thermal image analysis for machine fault diagnosis. *Proceedings of Prognostics and Health Management Conference*, pp. 1-6.

Zu, Y. K., Tian G. Y., Lu R. S. & Zhang H. (2011). A Review of Optical NDT Technologies. *Sensors, 11,* pp 7773-7798, www.mdpi.com/journal/sensors

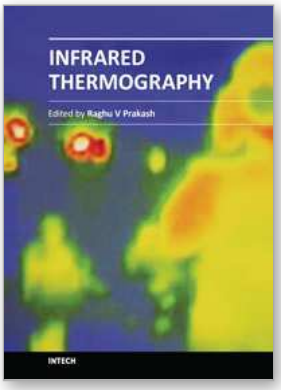

Infrared Thermography

Edited by Dr. Raghu V Prakash

ISBN 978-953-51-0242-7
Hard cover, 236 pages
Publisher InTech
Published online 14, March, 2012
Published in print edition March, 2012

Infrared Thermography (IRT) is commonly as a NDE tool to identify damages and provide remedial action. The fields of application are vast, such as, materials science, life sciences and applied engineering. This book offers a collection of ten chapters with three major sections - relating to application of infrared thermography to study problems in materials science, agriculture, veterinary and sports fields as well as in engineering applications. Both mathematical modeling and experimental aspects of IRT are evenly discussed in this book. It is our sincere hope that the book meets the requirements of researchers in the domain and inspires more researchers to study IRT.

How to reference

In order to correctly reference this scholarly work, feel free to copy and paste the following:

Soib Taib, Mohd Shawal Jadin and Shahid Kabir (2012). Thermal Imaging for Enhancing Inspection Reliability: Detection and Characterization, Infrared Thermography, Dr. Raghu V Prakash (Ed.), ISBN: 978-953-51-0242-7, InTech, Available from: http://www.intechopen.com/books/infrared-thermography/thermal-imaging-for-enhancing-inspection-reliability-detection-and-characterization

INTECH
open science | open minds

InTech Europe
University Campus STeP Ri
Slavka Krautzeka 83/A
51000 Rijeka, Croatia
Phone: +385 (51) 770 447
Fax: +385 (51) 686 166
www.intechopen.com

InTech China
Unit 405, Office Block, Hotel Equatorial Shanghai
No.65, Yan An Road (West), Shanghai, 200040, China
中国上海市延安西路65号上海国际贵都大饭店办公楼405单元
Phone: +86-21-62489820
Fax: +86-21-62489821